

CURRENT IDEAS FOR A CENTRAL TRACKER FOR EAGLE
USING MICROSTRIP GAS AVALANCHE CHAMBERS

C.A. AMERY, S.F. BIAGI, P.S.L. BOOTH , M. A. HOULDEN,
J.N. JACKSON, T. JONES, A. MORETON, N.A. SMITH

UNIVERSITY OF LIVERPOOL

MSGC detectors are a very promising technology for use in the high rate and high radiation environment of LHC. In this note we describe our current ideas on how to construct a barrel type detector for EAGLE using MSGCs in a two superlayer geometry. This initial design requires detailed examination on several issues, chief among which are pattern recognition capability and cost as well as the research and development of the MSGC technology. These studies are now underway and will provide the basis for a solution about the minimum number of space points required. We consider the design shown here as very much a first attempt which is probably on the conservative side as regards pattern recognition capability.

The following topics are discussed:-

- 1) Advances in detector development
- 2) A possible detector geometry
- 3) Electronics
- 4) Occupancies - effects of angled tracks
- 5) Pattern recognition
- 6) Resolutions
- 7) Trigger capability
- 8) Mechanical construction
- 9) Cost estimates (very preliminary)

1) ADVANCES IN DETECTOR DEVELOPMENT

There is currently a large R and D effort on substrates, electrode geometries and electronic read out at several laboratories including Bratislava, CERN, Liverpool, NIKHEF, RAL and Pisa. Several substrates have been investigated including glass, quartz and a SiO₂ layer on a silicon base. The necessary resistivity of the substrate may be achieved by impregnation with boron ions.

For example Angelini et al. (INFN PI/AE 91/90) have used a substrate of Si with a thin SiO₂ layer impregnated with boron ions and achieve stable operation as well as detecting a signal from back electrode. At Liverpool we are currently studying similar surfaces as well as glass substrates. Fig. 1 shows an early pulse height spectrum using a ⁵⁵Fe source achieved with a silicon substrate using an argon / DME gas mixture. The use of thin substrates should allow the design of a detector measuring two coordinates for one gas gap.

2) A POSSIBLE DETECTOR GEOMETRY

The concept is to construct a tracking detector by overlapping detectors in ϕ (~5% overlap) setting the angle of detectors at $\sim 15^\circ$ to compensate for Lorentz angle effects. The detector is constructed from 'planks' formed from a sandwich of a light support material carrying MSGC detectors so that each 'plank' contains ϕ , u and v planes. So far we have studied a Nomex honeycomb with a carbon fibre skin as the support material. Other possibilities such as SiC / B₄C foams are being investigated. The aim is to keep deflections under gravity to $< 100 - 200 \mu\text{m}$ over the length of the barrel.

A single barrel will consist of a series of overlapping planks and a complete inner or outer superlayer will consist of a number of these barrel layers. The lower limit on the number of layers will be determined by pattern

recognition requirements consistent with an acceptable overall cost for the complete tracking detector. To begin such a study each superlayer was assumed to consist of 5 barrel layers. At present we believe that this may reduce to at most 4 barrel layers for the inner superlayer and 3 barrel layers for the outer superlayer.

GENERAL STRUCTURE

A barrel layer will be constructed from “planks” orientated to compensate for the Lorentz angle with an overlap in azimuth. The complete superlayer will be constructed using a structure of interlocking wedges as shown in Fig 2 in order to maximise stiffness and minimise the material thickness.

Each plank consists of a sandwich two detectors thick mounted on layers of Nomex/carbon fibre. The complete detector is located within two concentric cylinders of 2 cm thickness formed from Nomex with carbon fibre skins. An example of the structure of an inner superlayer with 5 barrel layers is shown in Fig. 3

The detectors will be based on a suitably thin substrate eg. Si or 80 μm glass allowing back plane read out. The ϕ coordinate will be obtained from anode read out (200 μm pitch) and the z coordinate from u and v strips 1mm wide on the back plane arranged at angles of $\pm 45^\circ$ to the ϕ strips. Each detector will have a size of 20 cm x 15 cm with 750 ϕ strips and 350 u or v strips on the back plane at maximum. The electronics and connectors will be mounted on a 2 cm wide ‘L’ shape adjoining the active area. This means that there will be a 2 cm dead space between adjacent detectors along the beam direction but this region will be covered by the other detectors in the barrel layer because of the ‘brick wall’ structure as shown in Fig 4. The other electronic and connector area will be covered by the overlap in ϕ . The structure will be a ϕ u detector with a ϕ v detector mounted behind it. The detectors are so arranged to ensure that there will always be at least one space point from each plank. In fact the mean number of space points per track ~ 9 .

INNER SUPERLAYER

The number of barrel layers will be 5 at maximum and probably 4. The barrel layers are centred on radii of 400,440,480 and 520mm. The modularity of the plank structure is 28. This is determined by the available widths for the detectors and the Lorentz angle.

The anode spacing will be 200 μ m with 1mm u and v strips orientated at $\pm 45^\circ$. The space point accuracy is expected to be $\sigma_\phi \sim 40 \mu\text{m}$ and $\sigma_z \sim 400 \mu\text{m}$ (at $\eta \sim 0$).

Assuming a detector with 4 barrel layers the total number of detector tiles required is 1400 and the total number of electronic channels is ~ 1.2 M. Assuming 2mW per channel of electronics the total heat load for the detector is ~ 2.4 kW. The total thickness of material at $\eta \sim 0$ is $\sim 7\%$ of a radiation length (not accounting for overlapping planks).

OUTER SUPERLAYER

The outer superlayer uses the same construction technique with a modularity of 56. Again the maximum number of barrel layers was taken to be 5 although we now think that 3 would be adequate. These would be situated at radii of 900 mm, 940 mm, and 980 mm.

It is proposed to use 300 μ m spacing for anodes and 2mm wide u / v strips at this radius. For this case we expect space points with accuracy $\sigma_\phi \sim 60 \mu\text{m}$ and $\sigma_z \sim 800 \mu\text{m}$ (at $\eta \sim 0$).

Since the occupancy at this radius is reduced by approximately a factor of 4 we propose to bond two adjacent detectors together to give 400mm long anodes thus reducing the number of electronic channels. The resulting occupancy (NPC > 2) and B=2T is 1.3%.

The estimated number of detector tiles for a 3 barrel layer system is 4368 and the corresponding number of electronic channels is 1.4M. This would

produce an estimated heat load of ~ 2.8 kW.

3) ELECTRONICS

There are strong reasons for favouring analogue read out. The occupancy of the detector cells is a strong function of the discrimination cut on the pulse height as is demonstrated in section 4. It would be preferable to do this cut offline. Another advantage is the possibility of applying different thresholds off-line in the pattern recognition since high P_t tracks should give larger pulses than the slower curving tracks. This will provide a good starting point for pattern recognition. In addition the best position resolution obtained with these detectors makes use of charge sharing. This will be important when considering the momentum resolution of particles with momenta approaching the $1 \text{ TeV}/c^2$ range.

Another requirement is that the electronics should be able to tag the correct bunch crossing for a detector hit. Since width of the the detector signal is of order 3 bunch crossings such a facility will reduce background tracks by a factor of 3 and greatly simplify the pattern recognition problem. The RD20 approach to this problem seems to offer a promising solution for our purposes. Apart from a slightly different preamplifier the proposed solution of an analogue delay buffer with a APSP processor to flag the beam crossing and sparsification logic seems to be a good solution. The projected heat load is less than 2 mW per channel.

There will need to be additional electronics to read out the data. It obviously makes sense to have a degree of uniformity about how this is done throughout EAGLE. Our choice, using the same front end chip as the inner silicon tracker, is an example of this and we would propose to adopt the same read out solution as well. As well as introducing uniformity this approach may also lead to economies.

4) OCCUPANCIES AND ANGLED TRACK EFFECTS

INPUT ASSUMPTIONS

- 1) Anode spacing 200 μm ($\sigma \sim 40\mu\text{m}$)
- 2) Charge collection ~ 3 bunch crossings
- 3) Gas mixture Xe/DME/CO₂ (atmospheric pressure) giving
 - a) 11 primary clusters in a 3mm gas gap
 - b) a Lorentz angle of about 15^o depending on detailed mixture and electric fields
- 4) Maximum size for MSGCs of 20cm x 15cm
- 5) Magnetic fields of B=0.0,1.5 and 2T studied

SIMULATION

Minimum bias (including elastic) events were generated using PYTHIA at a luminosity $L=10^{34}\text{cm}^{-2}$ allowing 3 beam crossings (23.7 events/crossing).

Only charged tracks were considered.

A cylindrical detector with radius $R=50\text{cm}$ and length=120cm was divided into 6 detectors along its length giving 15710 x 6 anodes.

The path length in a 200 μm cell was calculated allowing for the angle of the track in both z and $r\phi$ in order to estimate the number of primary clusters per cell. Lorentz angle effects and diffusion of charge were not included.

Results for B = 0.0 T

- a) Occupancy = 0.32%
- b) The number of clusters generated has a mean of 13 in one cell giving an efficiency of 99.97% for a threshold set at number of clusters > 2 and 97.1% for number of clusters > 6
NB. Assumes one cell per track and neglects secondary statistics

Results for B = 1.5 T

- a) The P_t spectrum peaks ~ 0.25 GeV/c with $\langle P_t \rangle = 0.52$ GeV/c
- b) The angle of the track to the radius peaks at $\pm 12^\circ$ and ranges $\pm 90^\circ$
- c) The mean number of strips crossed per track was 6.08
- d) The mean number of primary clusters per cell was 2.06
- e) Apply a cut on NPC (number of primary clusters)=2,4,6

NPC	OCCUPANCY	<NO. STRIPS> /TRACK	EFF(1 cell hit)
-----	-----------	------------------------	-----------------

2	1.15%	3.67	99.97%
4	0.41%	1.31	99.5%
6	0.15%	0.49	97.

NB. Efficiencies are overestimates because of charge diffusion and Lorentz angle effects.

Results for $B = 2.0$ T

The results for a 2.0 T field vary very little from the 1.5 T case.

For example the cut at $NPC > 2$ gives a 1.2% occupancy.

The corresponding figure for a cell of $300\mu\text{m}$ spacing and 40cm length at a radius of $R=100$ cm is 1.3% occupancy.

5) PATTERN RECOGNITION

One of the critical areas in the design of a tracking detector is to ensure that it has good pattern recognition capability. This is especially true in the LHC environment. In order to begin assessing the problems we have developed a simple graphics program to display true space points. The space points are produced using PYTHIA. Higgs events are produced and the 4 muon decay is forced. This event is then overlaid with the minimum bias events expected in one (or more) bunches. The program allows cuts to be applied in both polar and azimuthal angles to simplify the display and allow pattern recognition by

eye. This work has just commenced at Liverpool with the immediate aim of convincing ourselves how many barrel layers are necessary in each superlayer.

Fig 5a and 5b show a typical event in both planes. Only one space hit is shown for each of the 5 barrel layers. Tracks from Higgs events are flagged as stars while those from minimum bias events are shown as crosses. Fig 5c shows the effect of applying simple angle cuts to this event and Fig 5d shows the same data using only 4 planes in the inner superlayer and 3 in the outer one. A second example of an event is shown similarly in Figs 6a-d. It can be seen that pattern recognition is possible by eye. The VERY preliminary conclusion is that pattern recognition is possible and probably only 4 inner barrel layers and 3 outer barrel layers will be necessary. Many more events need to be scanned with various physics processes such as those involving high energy jets in order to come to a final conclusion.

6) MOMENTUM RESOLUTION

The momentum resolution for two superlayers each with 5 barrel layers was studied. The maximum number of space points was taken to be 10 in each superlayer. The true space points were smeared assuming an accuracy $\sigma_\phi = 40 \mu\text{m}$ in the inner superlayer and $\sigma_\phi = 60 \mu\text{m}$ in the outer superlayer. A simple circle fit showed that the momentum accuracy assuming the beam spot as the vertex was $\Delta p/p = 1.4\%$ at $p=100\text{GeV}/c$.

7) A POSSIBLE TRIGGER

A $10 \text{ GeV}/c$ track passing through the outer layer makes an angle of 1.7° to the radius vector. In crossing the superlayer the track will change its $R\phi$ coordinate by $\sim 5 \text{ mm}$. A possible high P_t trigger may be formed by using an OR of ϕ anodes into strips $\sim 2 \text{ mm}$ wide and then trigger by demanding that 4/5 strips are hit in an "egg timer" shape as shown in Fig 7. This type of trigger has been used successfully in the DELPHI Outer Detector. A trigger is still feasible using this principle if the number of barrel layers is reduced to 3.

A detailed study of trigger efficiency and the additional electronics is needed.

8) MECHANICAL CONSTRUCTION

The general outline of the detector assembly is shown in Figs 2 and 3. The Nomex honeycomb with carbon fibre skins will need to be ordered from industry already shaped into sheets, cylinders and end pieces. Individual planks will be built up 'in house'. Special jigs will be required to position completed individual detectors (with electronics) accurately on one support sheet. A second sheet would then be attached and a the second layer of detectors positioned again using the jig. Positional accuracy of 20 μm will be required at this stage with the aim of a final measured alignment accuracy of 10 μm .

A second jig will be required to construct the 'wedges' consisting of individual planks linked together by carbon fibre pultrusions as shown in Fig. 3. Finally the complete detector would be assembled between the inner and outer cylinder. For simplicity we are considering using the whole volume of the vessel as a gas volume. The necessary ports for cables and cooling pipes require further detailed study.

9) COSTS

The question of cost is very difficult to address meaningfully until the overall design is closer to being frozen. A great deal will depend on the number of collaborating institutes and the amount of technical assistance available. For this reason we have for the moment restricted this discussion to the major cost components of such a detector and have not addressed the question of labour costs.

The fundamental building block consists of the MSGC tile together with the associated electronics. The cost of the tile depends on whether it is produced in industry or internally. The industrial cost for a glass tile of the size required is estimated to be ~ £300 based on the experience of ourselves and RAL. In addition to this the u / v planes require construction but this is a much easier task as high accuracy is not required. The cost should be

equivalent to processing a standard single sided PC board estimated as £10 . It is possible to reduce the cost per tile by undertaking the fabrication within the collaborating institutes. We intend to investigate this possibility since the potential exists to reduce the cost per tile by a large factor once a fabrication facility has been set up. For the present we simply quote the industrial cost.

The cost of the electronics per channel should be the same as that for the inner silicon tracker. Our estimate is based on the cost of the current MX3 chip as used in DELPHI of ~ £20 for 128 channels. The RD20 electronics would yield 64 channels in a chip of the same size. The assumed cost for radiation hard electronics is to scale by a factor between 2 and 3. In addition we will require one read out chip for each detector so we estimate the probable cost of the electronics as ~ £1 per channel.

The inner superlayer of 4 barrel layers consists of 1400 tiles with 1.15M electronic channels yielding a cost of £0.42M for the tiles and £1.15M for the electronics giving a total of £1.57M or ~4M SF.

The outer superlayer of 3 barrel layers consists of 4368 tiles with 1.41M electronic channels yielding a cost of £1.31M for the tiles and £2.05M for the electronics giving a total of £3.46M or ~8.7M SF.

These costs are summarised in the following table.

INNER SUPERLAYER		COST £k
ITEM		
1400 tiles		420
1400 back planes		14
1400 F/E and H/V boards		182
F/E electronics		1150
OUTER SUPERLAYER		COST £k
ITEM		
4368 tiles		1410
4368 back planes		44

2184 F/E and H/V boards	284
F/E electronics	3460

TOTAL £6.96M

CONSTRUCTION COSTS

ITEM	COST £k
Prototyping	50
Tooling (moulds, jigs etc)	250
Inner and outer endplates + supports	50
MSGC carrier strips	75
Materials, Pultrusions etc.	50
Gas and water cooling	45
Special machining	40
Transport, packing etc.	10
Contingencies	60

TOTAL FOR MECHANICAL CONSTRUCTION £630k

The total cost of both the inner and outer superlayers is £7.6M (19M CHF) . This estimate includes only the major expenses and contains a large factor of uncertainty mainly in the cost of the electronic components (67% of total) and in the cost of the basic detector tiles (25% of total). The cost for the tiles may be reduced by fabrication 'in house'. The cost for the electronic read out depends on the number of channels and the cost per channel, the latter being similar for most detectors in EAGLE. The cost of implementing a trigger has not been included.

FIGURE CAPTIONS

- FIG. 1 A preliminary pulse height spectrum from an ^{55}Fe source obtained using a SiO_2 substrate and an argon / DME gas mixture.
- FIG. 2 Construction of inner superlayer with 5 barrel layers.
- FIG. 3 End view of inner superlayer.
- FIG 4 Arrangement of detectors in a 'brick wall' structure.
- FIG 5 a Space points of a Higgs event + 1 beam crossing of minimum bias events at a luminosity of 10^{34} cms^{-2} in radial view.
- FIG 5 b Event in side on view.
- FIG 5 c A section of the radial view showing tracks with polar angles between 40° and 60° .
- FIG 5 d As in Fig 5c but showing only 4 barrel layers in the inner detector and 3 barrel layers in the outer detector.
- FIG 6 a-d As for fig.5 a-d showing another event. The polar angles selected are between 60° and 80° in this case.
- FIG 7 A sketch showing the 'egg timer' trigger scheme for a 5 layer system and a reduced version for a three layer system.

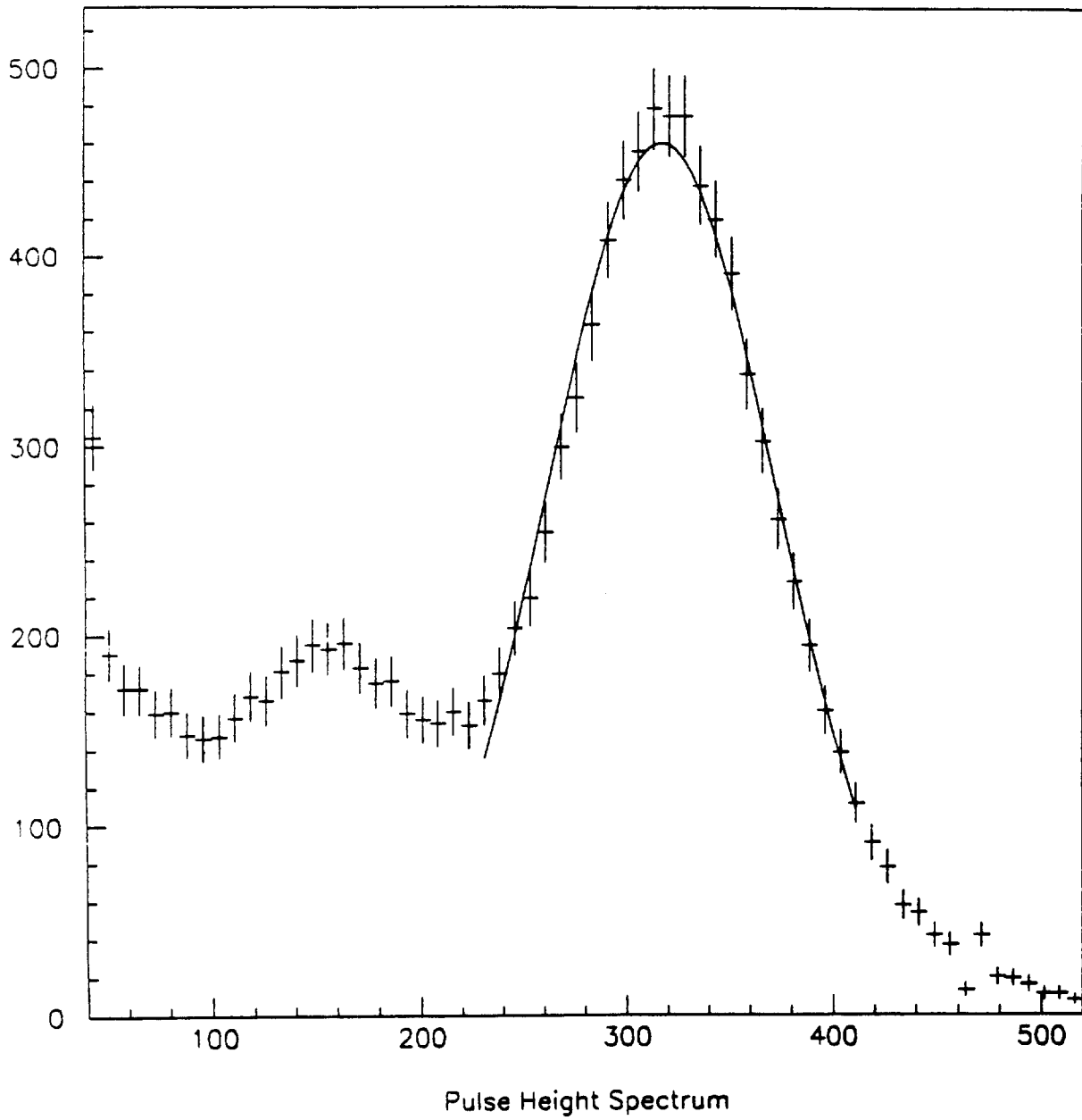


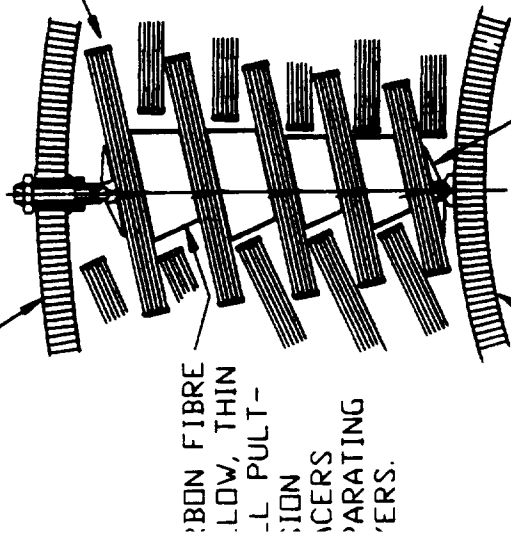
Fig 1

Fig 2

CARBON FIBRE PULTRUSION EDGE SEPERATING
PIECES UNITE THE 3 CARRIER STRIPS INTO A
STIFF LATTICE BEAM STRUCTURE.

CARBON FIBRE/NOMEX HONEYCOMB
UTER CYLINDER.

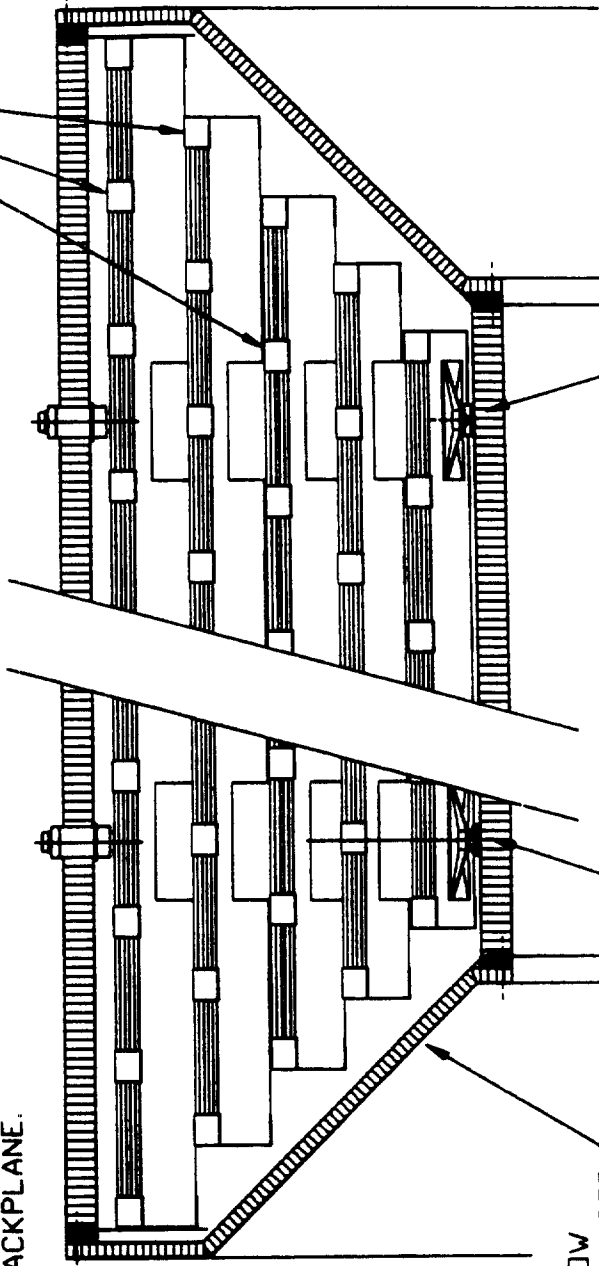
EACH DETECTOR LAYER CONSISTS OF 3 CARRIER STRIPS OF 3mm THICK CARBON
FIBRE/NOMEX HONEYCOMB MADE INTO A STIFF COMPOSITE BY MEANS OF INTER-
MITTENT CARBON FIBRE PULTRUSION EDGE SPACING PIECES BONDED TOGETHER IN A JIG.
THE INNER CARRIER SUPPORTS A LINE OF SINGLE SIDED MISGACS AND THE MIDDLE
CARRIER A LINE OF DOUBLE SIDED MISGACS. THE THIRD CARRIER IS ONLY FOR
SUPPORTING THE BACKPLANE.



CARBON FIBRE
LOW, THIN
PULTRU-
SION
PIECES
SEPARATING
CARRIERS.

HIGH STRENGTH, LOW
DENSITY POLYMERS USED
FOR ALL SUPPORTS.

CARBON FIBRE/NOMEX HONEYCOMB
INNER CYLINDER.



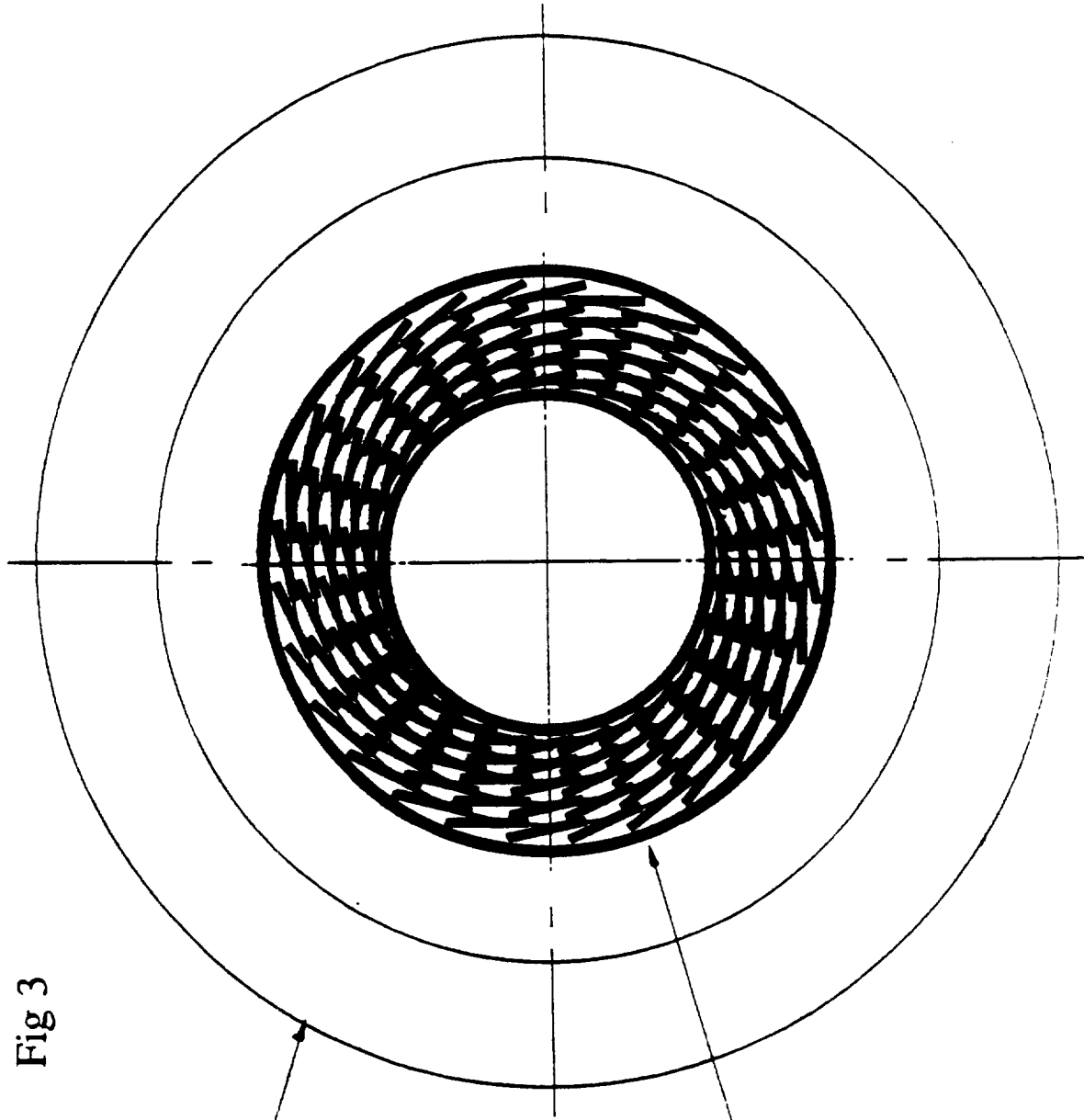
CARBON FIBRE/
NOMEX HONEYCOMB
ENDPLATES.

LOCATION IN R, Ø AND Z.

LOCATION IN R AND Ø WITH
FREEDOM TO FLOAT IN Z.

PART TRANSVERSE AND AXIAL SECTION THROUGH A FIVE LAYER PLANK
IN THE INNER DETECTOR WITH SOME SUGGESTIONS FOR CONSTRUCTION

Fig 3



OUTER CENTRAL TRACKER IS
SIMILAR TO INNER CENTRAL
TRACKER EXCEPT THAT THE
MODULARITY IS 56.

INNER CENTRAL TRACKER
HAS A MODULARITY OF 28
AND CONSISTS OF 5 LAYERS
OF DETECTORS,

ARGE HADRON COLLIDER -- SECTION THROUGH INNER AND OUTER CENTRAL TRACKER

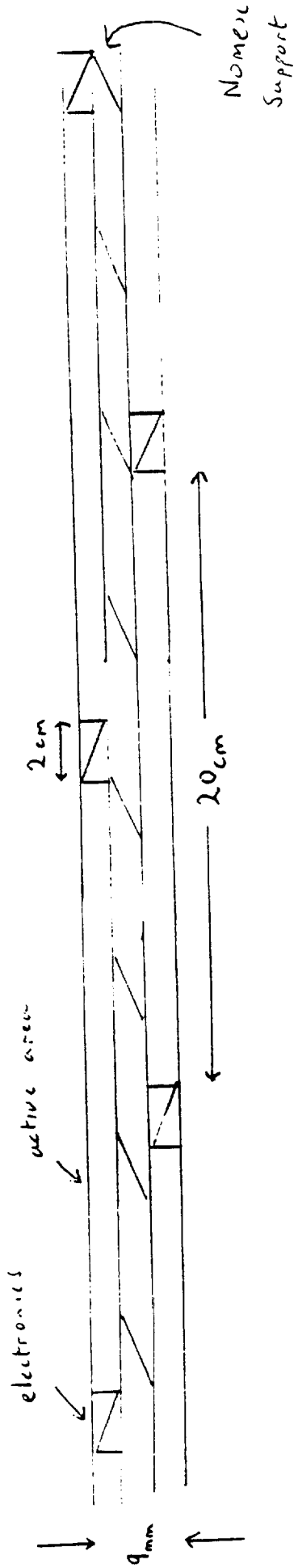


Fig 4

EVENT 1 HGZ+1BC

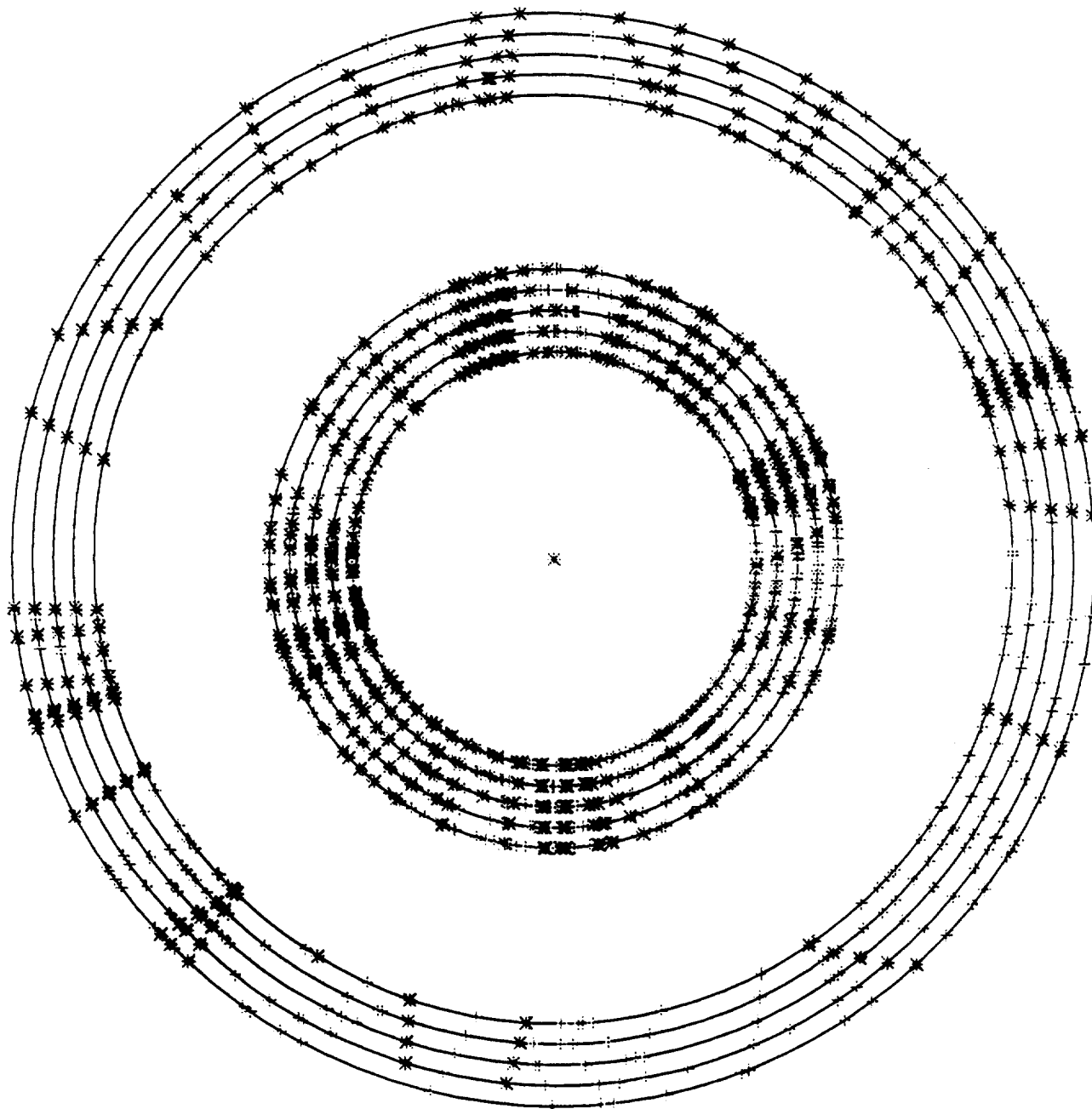


Fig 5a

EVENT 1 HGZ+1BC

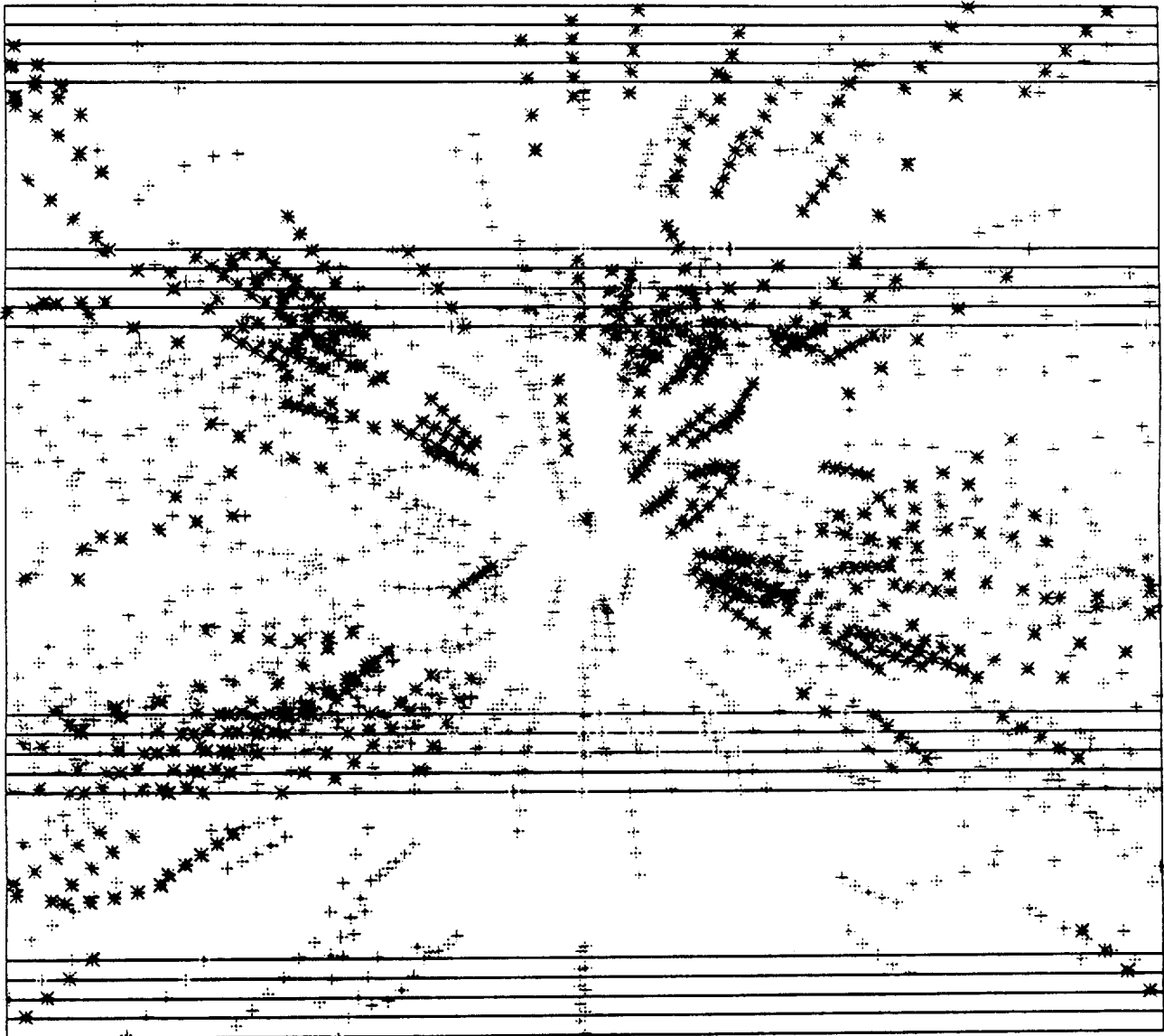
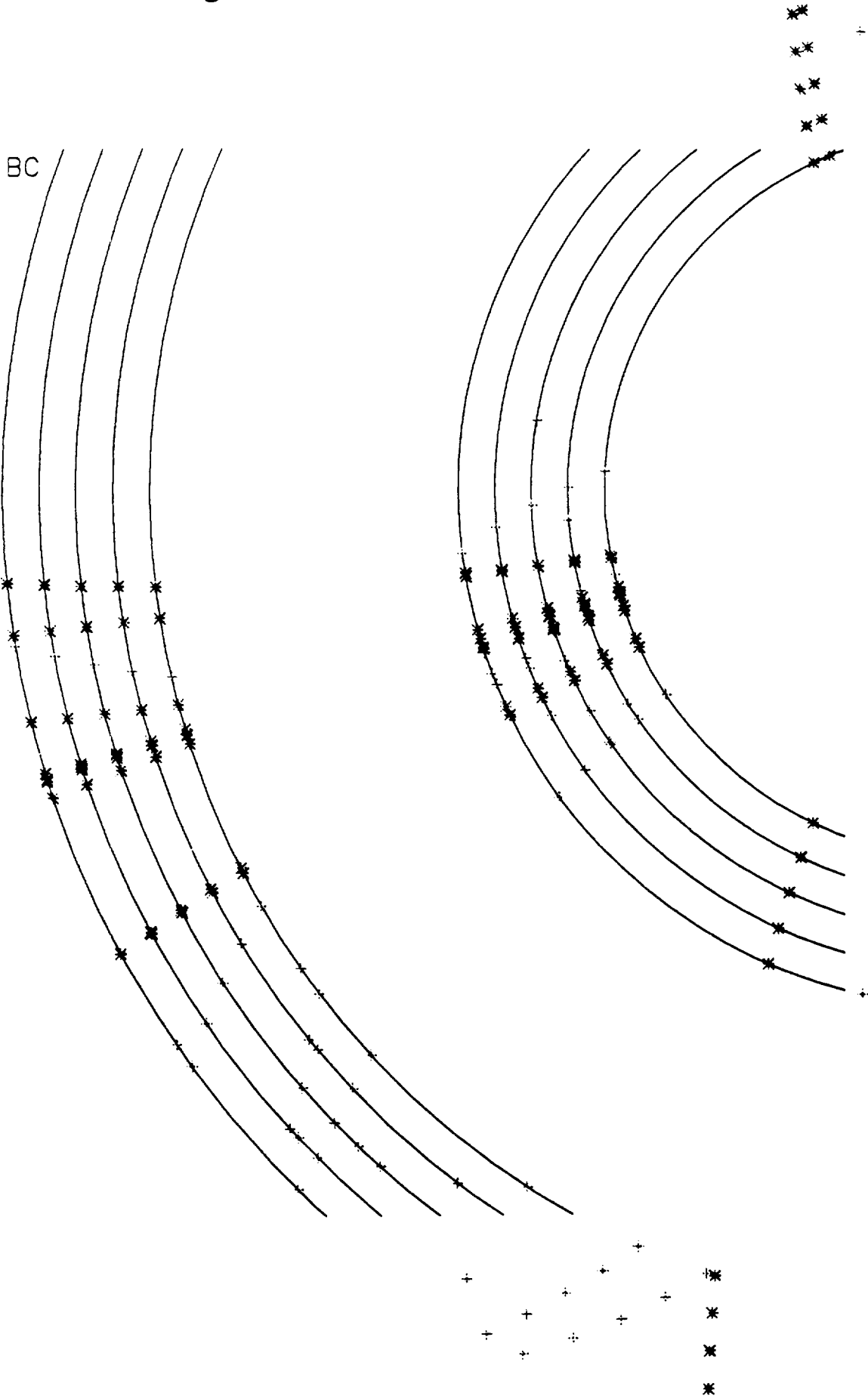


Fig 5b

Fig 5c

EVENT 1 HGZ+1BC
THETA 40-60



EVENT 1 HGZ+1BC
THETA 40-60

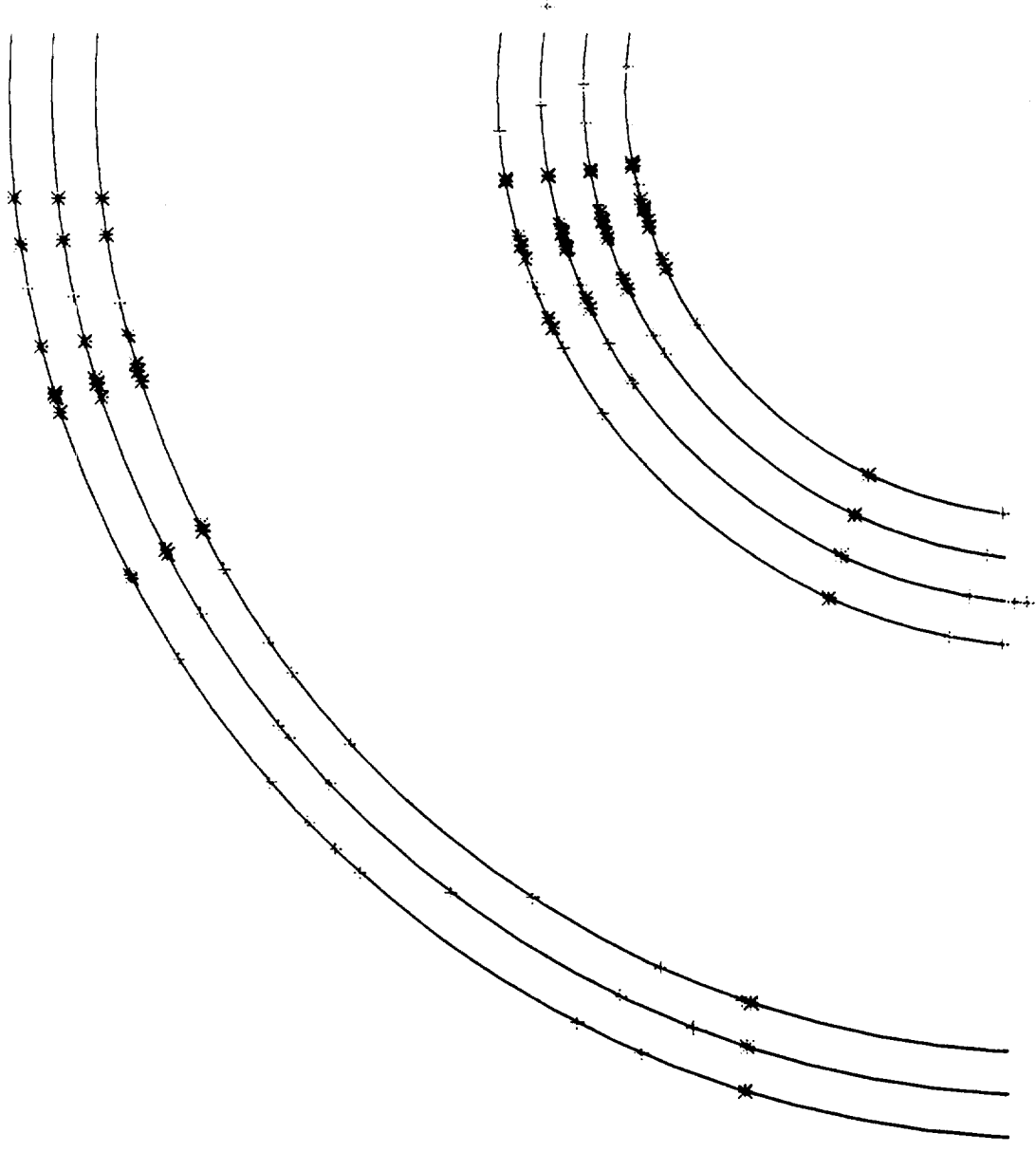


Fig 5d

EVENT 3 HGZ+1BC

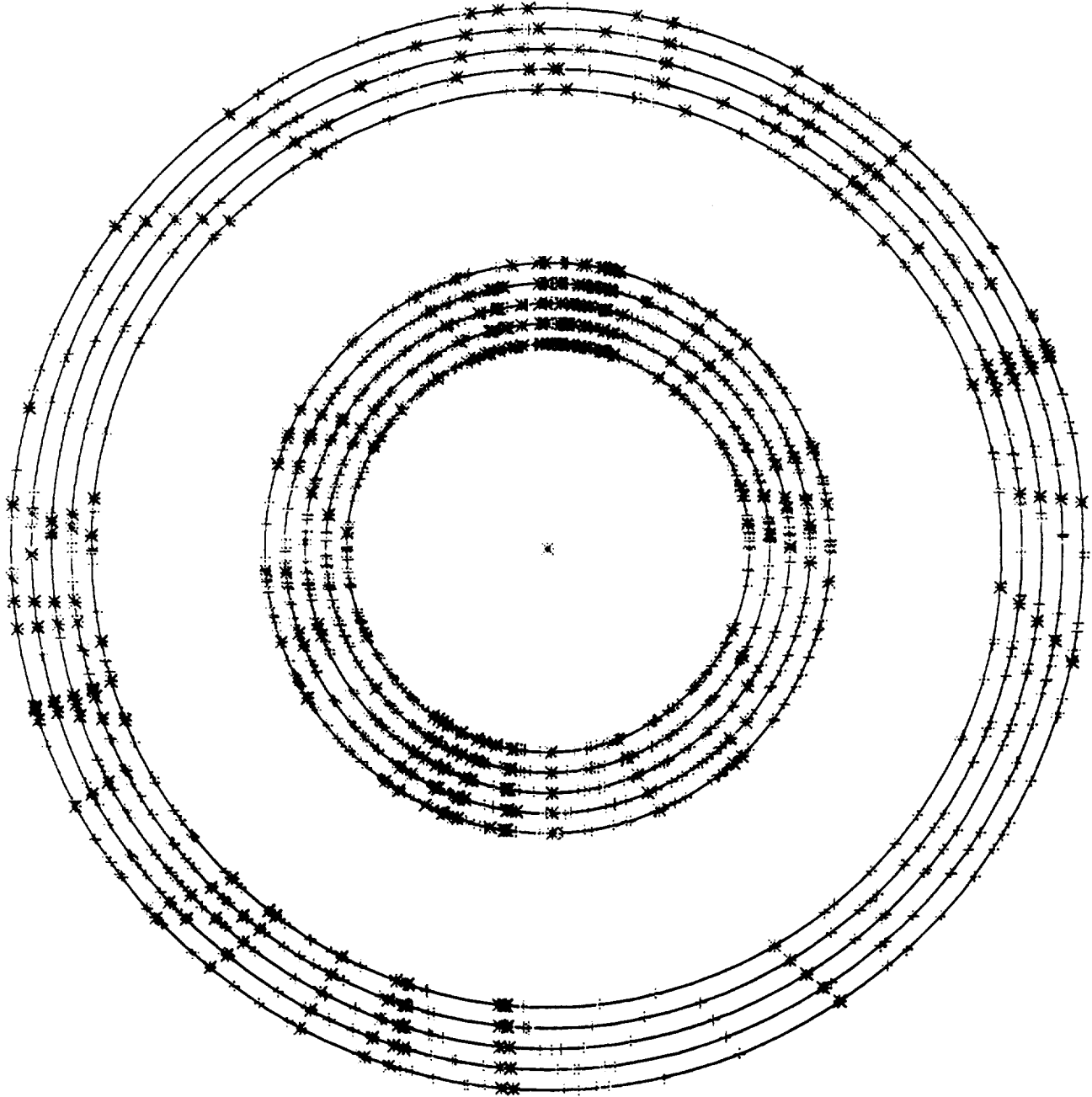


Fig 6a

EVENT 3 HGZ+1BC

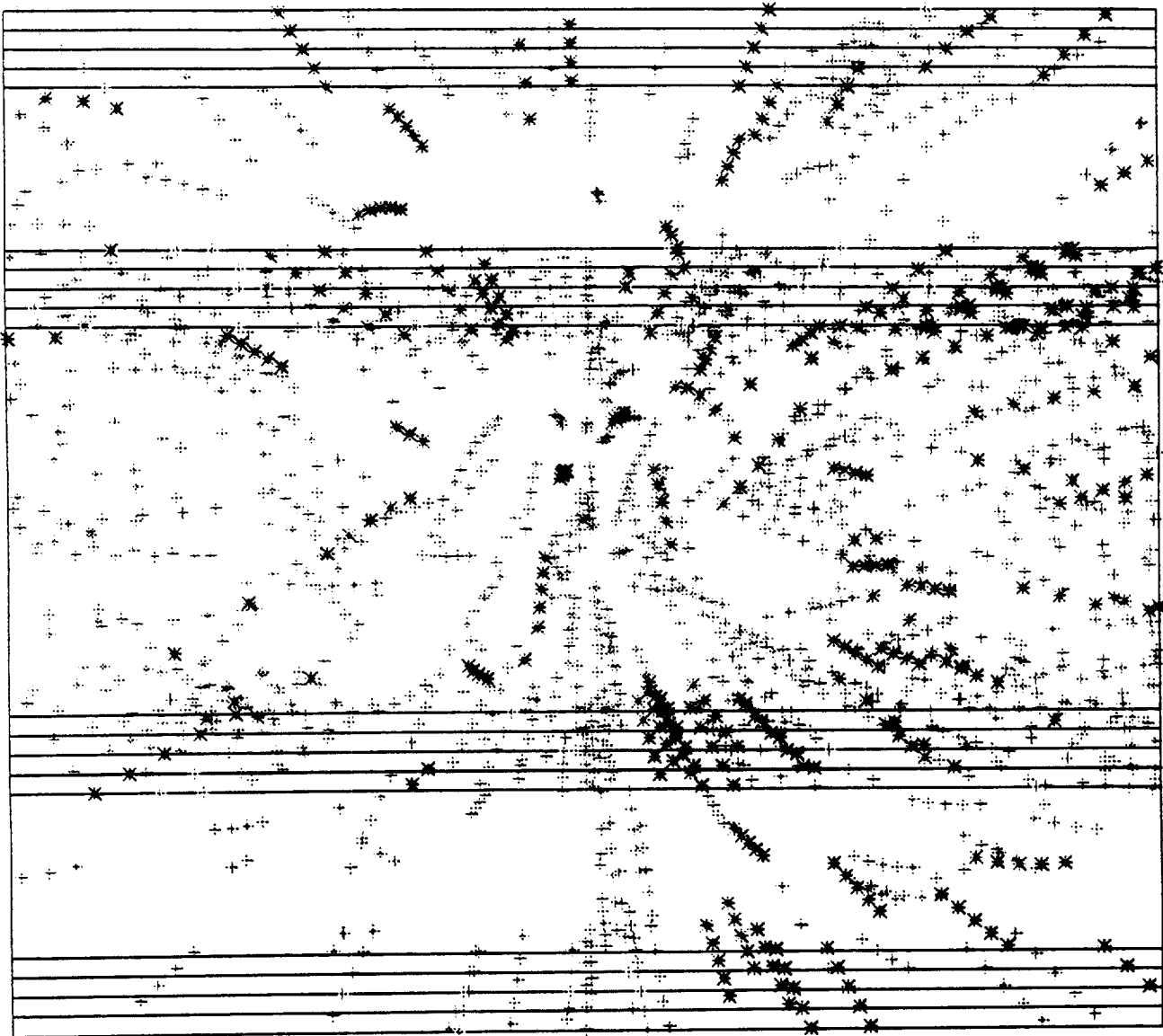


Fig 6b

EVENT 3 | HGZ+1BC
THETA 60 - 80

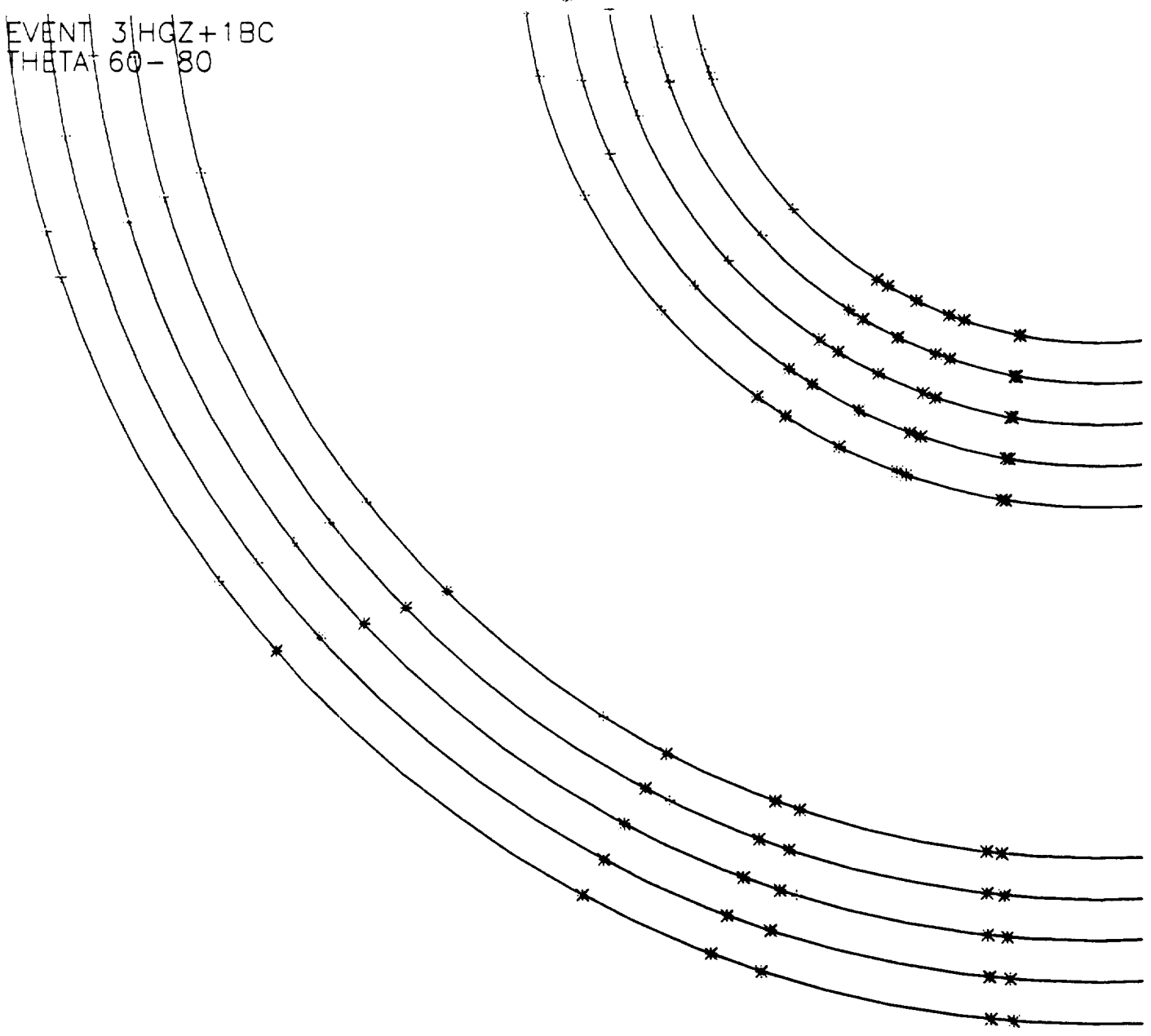


Fig 6c

EVENT 3 HGZ+1BC
THETA 60-80

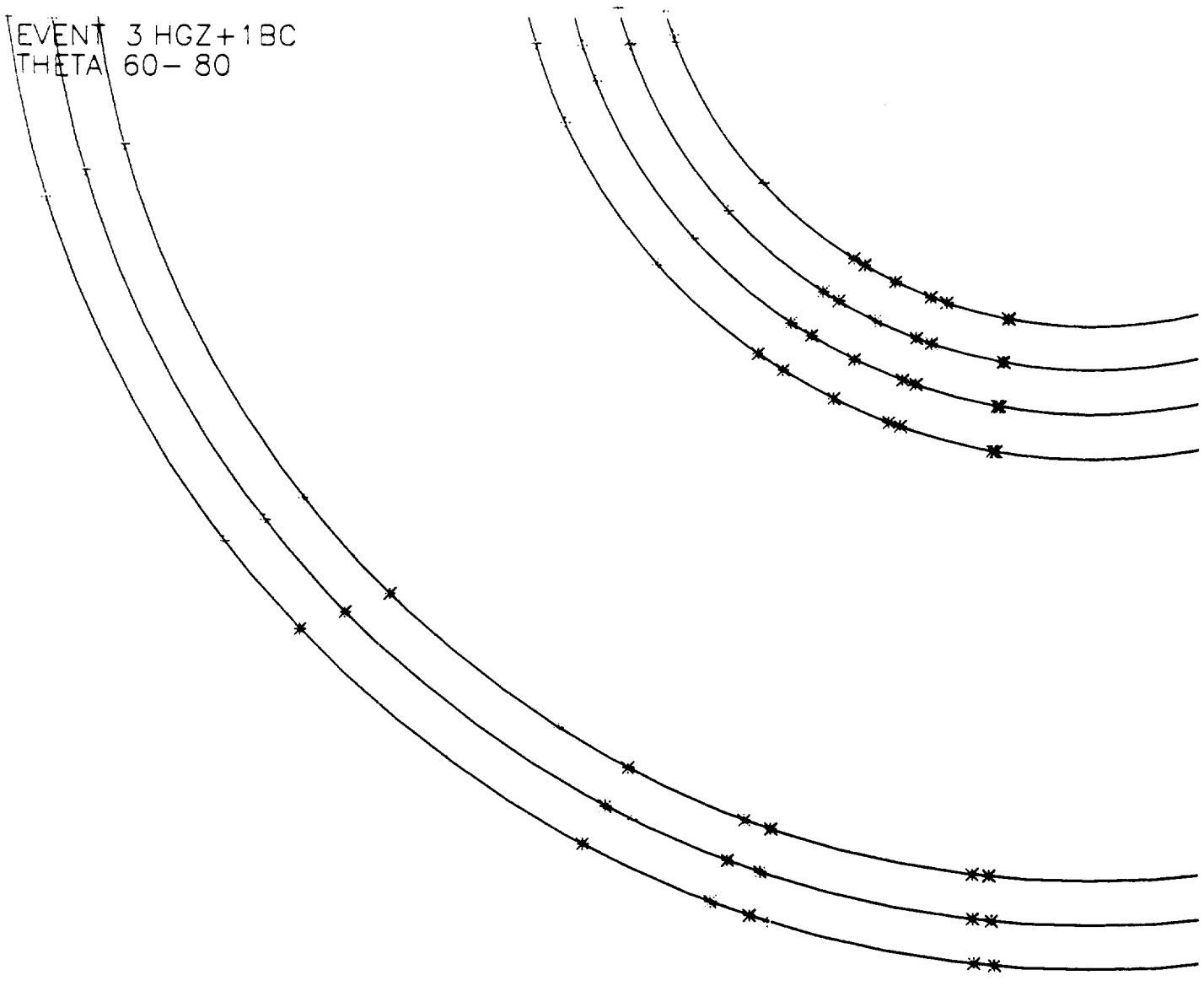


Fig 6d

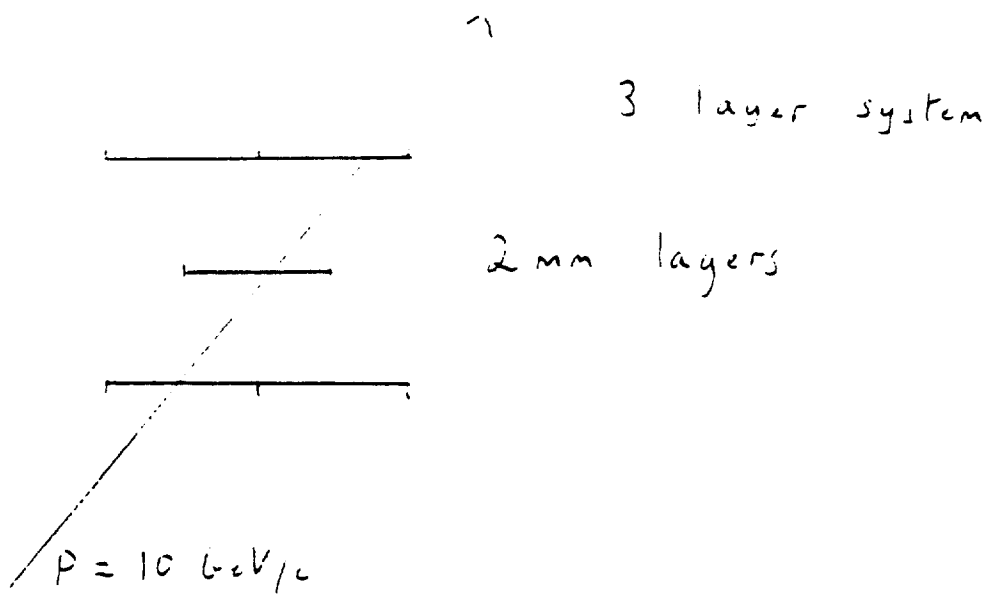
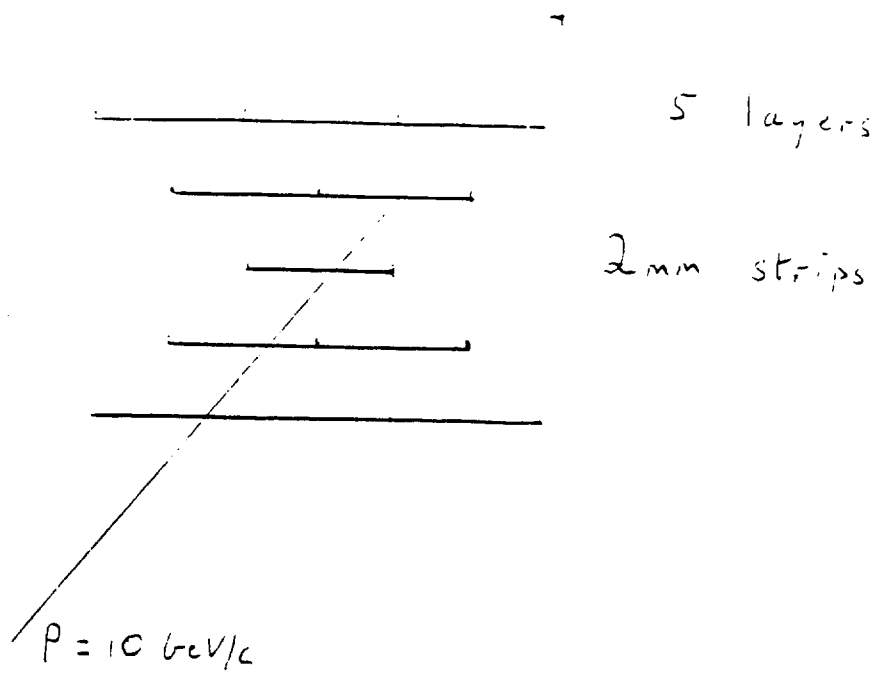


Fig 7